Hydrological effects on carbon cycles of Canada's forests and wetlands

By WEIMIN JU[1]*, JING M. CHEN[1], T. ANDREW BLACK[2], ALAN G. BARR[3], HARRY MCCAUGHEY[4] and NIGEL T. ROULET[5],   [1]*Department of Geography, University of Toronto, Toronto, Ontario, Canada 100 St. George St., Room 5047, Toronto, Ontario, Canada M5S 3G3;* [2]*Department of Agricultural Science, University of British Columbia, Vancouver, BC, Canada;* [3]*Climate Research Branch, Meteorological Service of Canada, Saskatoon, SK, Canada;* [4]*Department of Geography, Queen's University, Kingston, Ontario, Canada;* [5]*Department of Geography, Center for Climate and Global Change Research, McGill University, Montreal, Quebec, Canada*

ABSTRACT

The hydrological cycle has significant effects on the terrestrial carbon (C) balance through its controls on photosynthesis and C decomposition. A detailed representation of the water cycle in terrestrial C cycle models is essential for reliable estimates of C budgets. However, it is challenging to accurately describe the spatial and temporal variations of soil water, especially for regional and global applications. Vertical and horizontal movements of soil water should be included. To constrain the hydrology-related uncertainty in modelling the regional C balance, a three-dimensional hydrological module was incorporated into the Integrated Terrestrial Ecosystem Carbon-budget model (InTEC V3.0). We also added an explicit parameterization of wetlands. The inclusion of the hydrological module considerably improved the model's ability to simulate C content and balances in different ecosystems. Compared with measurements at five flux-tower sites, the model captured 85% and 82% of the variations in volumetric soil moisture content in the 0–10 cm and 10–30 cm depths during the growing season and 84% of the interannual variability in the measured C balance. The simulations showed that lateral subsurface water redistribution is a necessary mechanism for simulating water table depth for both poorly drained forest and peatland sites. Nationally, soil C content and their spatial variability are significantly related to drainage class. Poorly drained areas are important C sinks at the regional scale, however, their soil C content and balances are difficult to model and may have been inadequately represented in previous C cycle models. The InTEC V3.0 model predicted an annual net C uptake by Canada's forests and wetlands for the period 1901–1998 of 111.9 Tg C yr^{-1}, which is 41.4 Tg C yr^{-1} larger than our previous estimate (InTEC V2.0). The increase in the net C uptake occurred mainly in poorly drained regions and resulted from the inclusion of a separate wetland parameterization and a detailed hydrologic module with lateral flow in InTEC V3.0.

1. Introduction

The terrestrial carbon (C) and water cycles interact at various temporal and spatial scales (Ball et al., 1987; Rodriguez-Iturbe, 2000; Arain et al., 2002; Blanken and Black, 2004). The water cycle plays a key role in the control of stomatal conductance (Jarvis, 1976; Lhomme et al., 1998; Harris et al., 2004) and microbial activity (Parton et al., 1993), and therefore the C balances of terrestrial ecosystems (Rodriguez-Iturbe, 2000). Canopy photosynthesis and soil organic C decomposition are very sensitive to soil moisture content in the root zone. A small change in soil moisture content can have a large effect on the rates of C assim-

ilation, heterotrophic respiration, and consequently net ecosystem production. Drought has different effects on net forest C exchange. Based on multi-year, eddy-correlation flux measurements of CO_2 and climate data obtained at extensive stands of old aspen (SOA), old black spruce (SOBS), and old jack pine (SOJP) at the Boreal Ecosystem-Atmosphere Study Southern Study Area (BOREAS SSA)/Boreal Ecosystem Research and Monitoring Sites (BERMS) super site near Prince Albert National Park, Saskatchewan, Canada, Kljun et al. (2004) found that drought had significant effects on net C exchange at the deciduous site whereas the conifer stands showed very limited reaction to drought. Daily gross ecosystem productivity (GEP) of SOA in July and August of 2003 decreased from 12 g to only 6 g C m^{-2} d^{-1} after 3 yr of drought conditions. In contrast, the SOJP and SOBS stands showed modest reductions in GEP of 2 g C

*Corresponding author.
e-mail: juw@geog.utoronto.ca

m^{-2} d^{-1} in August of 2003 (GEP approximately 5 and 6 g C m^{-2} d^{-1} in non-drought years). The reductions in GEP were partially offset by reduced ecosystem respiration when the soil moisture content was low. A northern peatland, Mer Bleue (MB), East of Ottawa, Ontario, Canada exhibited a modest response of GEP to drought similar to that observed in SOBS and SOJP (Humphreys et al., 2004). Based on model simulation, D'odorico et al. (2003) concluded that an accurate representation of hydrological mechanisms was necessary to capture the impact of high-frequency variability of soil moisture content on N and C dynamics.

A reliable simulation of soil moisture content is a prerequisite for reliable estimates of the regional C balance. In recent decades, a variety of terrestrial ecosystem models have been developed to simulate the C, nutrient (N), energy and water cycles at global and regional scales, embracing terrestrial biogeochemistry (Running and Gower, 1991; Parton et al., 1993; Potter et al., 1993; Friend et al., 1997; Potter, 1997; Chen et al., 2000a; Frolking et al., 2002), global and regional vegetation biogeography (Neilson and Marks, 1994; Neilson, 1995; Haxeltine and Prentice, 1996; Kucharik et al., 2000), and land–atmosphere exchange processes (Dickinson et al., 1986; Sellers et al., 1986, 1996; Bonan et al., 2003). These models employ different algorithms to describe the hydrological cycle, ranging from one-layer, linear drying bucket models to multi-layer, non-linear drying models (BIOME3, Haxeltine and Prentice, 1996; CENTURY, Parton et al., 1993; Hybird 3.0, Friend et al., 1997; IBIS, Kucharik et al., 2000; MAPSS, Neilson, 1995; NASA-CASA, Potter et al., 1993; Potter, 1997, 1999; Potter et al., 2001; SiBs, Sellers et al., 1986, 1996; and TEM, Raich et al., 1991; McGuire et al., 1992). These models describe in detail the vertical movement of water in soil and the exchange of water between terrestrial ecosystems and the atmosphere. However, none of these published models includes the mechanistic horizontal redistribution of soil water. This exclusion is questionable, especially in complex terrain (Soulis et al., 2000), because it can cause the underestimation of soil moisture content and consequently soil C content in water-convergent regions. The distribution of soil moisture content is influenced by topographic factors (Qiu et al., 2001), including slope (Moore et al., 1988), aspect (Western et al., 1999), curvature (Western et al., 1999), slope position, and relative elevation (Grayson et al., 1997). Using a distributed hydrological model at the BOREAS/BERMS SOBS site, a flat area with less than 1.5 m of topographical variation over a radius of 150 m, Chen et al. (2005) estimated a water loss of 10.5 mm through lateral saturated subsurface flows during the growing season of 1994, accounting for 5.7% of the rainfall in the same period. Su et al. (2000) estimated that a wetland in the St. Denis National Wildlife Area, 45 km East of Saskatoon, received mean annual runoff of 206 mm from the surrounding uplands over a 28-yr simulation period, equivalent to about 60% of annual precipitation.

Wetlands, presently covering 127 million hectares or 14% of the landscape of Canada, play an important role in the terres-

trial C cycle (Frolking et al., 1998). In spite of their low primary productivity, these ecosystems have been continuously accumulating C at an average rate of 20–30 g C m^{-2}yr^{-1} over the past 5000–10 000 yr (Tolonen et al., 1992; Gorham, 1995; Rapalee et al., 1998). The net C accumulation is caused by very slow decomposition rates of soil organic matter, which are in turn related to the resistance of the litter to decomposition, the anaerobic condition within the saturated peat profile, and the generally low temperatures of peat due to the large heat capacities and the low thermal conductivity of the moss cover (Roulet et al., 1997). The most critical factor in determining the wetland's role as a source or sink of C appears to be the wetness (Oechel et al., 1993; Silvola et al., 1996; Lafleur et al., 2003). The strong dependence of the decomposition of soil organic matter on soil moisture content and temperature makes the C balance in northern wetlands very sensitive to disturbance and climate change (Alm et al., 1999; Soegaard and Nordstroem, 1999; Baron et al., 2000). These regions have experienced significant increases of temperature in the past 100 yr (Gagnon and Gough, 2002) and could become much warmer and possibly drier in the future (Gough and Wolfe, 2001). The projected climate change is expected to alter the hydrology of these regions and may shift the net C balance from sink to source. Northern wetlands are often ignored in regional- and global-scale ecosystem and climate models that do not resolve small surface features (Frolking et al., 1998; Moore et al., 1998). Many models represent wetlands as upland forests, diminishing the reliability of the estimated regional C balance at high latitudes due to the huge aggregated area of wetlands.

Working at 1-km spatial resolution, the InTEC model has the capacity to include spatially explicit wetlands with a unique wetland parameterization. This paper reports results from InTEC V3.0, a recent revision that includes an improved hydrological module and separate parameterizations for forests and wetlands. These changes have significantly improved the agreement between simulated soil C content and that compiled from the soil landscapes of Canada (SLC) database in Canadian forests and wetlands (Ju and Chen, 2005). The main objectives of this paper are: (1) to examine the ability of this model to simulate soil moisture content, water table depth and interannual variability of C balance at representative flux-tower sites; (2) to investigate the effect of hydrology on soil C accumulation and the dependence of soil C content on drainage conditions and (3) to analyse the hydrology-related uncertainty in modelling regional terrestrial C balances through comparing net ecosystem productivity (NEP) results from two versions of InTEC, with and without the improved hydrological module and explicit wetland parameterization.

2. Model description

The InTEC model is a biogeochemical model to estimate annual forest C budgets at regional scales, driven by remotely sensed

vegetation parameters (such as leaf area index (LAI), land cover type, stand age), climate, and soil texture. It is a combination of a modified CENTURY model for soil C and nutrient dynamics (Parton et al., 1987, 1993), and a canopy-level annual photosynthesis model developed from Farquahar's leaf biochemical model (Farquhar et al., 1980) using a temporal and spatial scaling scheme (Liu et al., 1999; Chen et al., 1999b, 2000a). The formulations and applications of this model can be found in Chen et al. (2000a, 2003). Here, we only outline the major characteristics of the InTEC model.

The historical annual net primary productivity (NPP) is progressively calculated using an iterative approach (Chen et al., 2000a, 2003), that is,

$$\text{NPP}_i = \text{NPP}_o \frac{F(a_i)}{F(a_o)} \prod_{j=1}^{i} \frac{2+\chi(j)}{2-\chi(j)}, \tag{1}$$

where NPP_i is the simulated NPP in the ith year; NPP_0 is the initial value of NPP in the starting year; $F(a_i)$ and $F(a_o)$ are normalized productivity of a forest at ages a_0 (the starting year) and a_i (the ith year), respectively, (Chen et al., 2003); $\prod_{j=1}^{i} \frac{2+\chi(j)}{2-\chi(j)}$ is the integrated effects on NPP of non-disturbance factors including climate, CO_2 fertilization and N availability (Chen et al., 2000a).

The annual NPP in 1994, estimated at daily time steps using the Boreal Ecosystems Productivity Simulator (BEPS) model (Liu et al., 2002), is used as a benchmark to tune the value of NPP_0. For each pixel, the value of NPP_0 is repeatedly adjusted until the difference between NPP from InTEC and that from BEPS in 1994 is smaller than a threshold, typically, $\pm 1\%$. The land cover map derived from remote sensing (Cihlar et al., 1998) is used to determine model parameters, such as coefficients allocating NPP into foliage, wood, fine root, and coarse root biomass C pools, and litter quality (lignin content) (Chen et al., 2003). The modified soil sub-model of CENTURY (Parton et al., 1993) is employed to simulate soil C and N dynamics. The major modifications to the original CENTURY model include: (1) in addition to foliage and fine root litter pools, a woody litter pool is added; (2) the soil temperature effect on decomposition is quantified using a modified Arrhenius-type equation (Lloyd and Taylor, 1994; Chen et al., 1999a); (3) the modifier for the effect of soil moisture content on decomposition is a function of the fraction of water-filled pore space (defined as the ratio of volumetric soil moisture content (VSMC) to total porosity of the soil) (Potter, 1997); (4) the maximum decomposition rate of slow and passive C pools is related to drainage class; (5) the rate of N fixation from the atmosphere is a function of temperature, precipitation, and the size of microbial pool (Chen et al., 2000b) and (6) the N deposition rate is spatially and temporally interpolated based on measured N deposition rates at 29 stations during the period 1983–1994 and historical greenhouse gas emission in Canada (Chen et al., 2003). The annual dynamics of the jth soil C pool

in the ith year is updated as:

$$\Delta C_{i,j} = \left[\sum_{m=1}^{n} \varepsilon_{m,j} K_{i,m} C_{i-1,m} - C_{i-1,j} K_{i,j} \right] \bigg/ (1 + K_{i,j}), \tag{2}$$

where $\varepsilon_{m,j}$ is the fraction of decomposed C transfer from the mth to the jth C pool; $K_{i,m}$ and $K_{i,j}$ are the decomposition rates of the jth and mth C pools in the ith year; $C_{i-1,m}$ and $C_{i-1,j}$ represent the sizes of the jth and mth C pools in the $(i-1)$th year. For each year and each pool, eq. (2) is used to compute the C transfers from and to all other pools.

The regional estimate of the annual C balance in upland forests and wetlands is the sum of NEP of each pixel, which equals the difference between NPP and heterotrophic respiration, that is,

$$\text{NEP}_i = \text{NPP}_i - R_{h_i} = \text{NPP}_i - \sum_{m=1}^{N} \tau_m K_{i,m} C_{i,m}, \tag{3}$$

where NEP_i and NPP_i are simulated NEP and NPP in the ith year, respectively; τ_m is C respiration efficiency, representing the percentage of decomposed C released from the mth pool to the atmosphere; N is the number of soil C and litter pools, which is equal to 9.

The decomposition of C in poorly drained soils generates CO_2, methane (CH_4) and dissolved organic carbon (DOC) (Potter, 1997; Frolking et al., 2002). Experimental studies suggest that the production ratio of CO_2 to CH_4 depends on the position of water table (Moore and Knowles, 1989; Funk et al., 1994; Potter, 1997). Conceptually, CH_4 is transported to the atmosphere through three pathways: molecular diffusion, ebullition, and plant vascular transport. The main purpose of the InTEC model is to estimate the regional C balance. For simplicity, we simulated the amount of C emitted to the atmosphere as a function of total C decomposed and C respiration efficiency regardless of whether the C is released as CO_2 or CH_4. DOC export depends significantly on hydrology (typically runoff) while temperature weakly affects DOC release (Moore et al., 1998). In our current model, C leaching is computed as a function of soil water drainage and texture following the CENTURY model (Parton et al., 1993).

In InTEC, all processes except the hydrological cycle are simulated at annual time steps. The hydrological module operates at monthly time steps to provide more realistic simulations of soil water and temperature dynamics for evaluating the effects of environmental conditions on heterotrophic respiration and NPP. Its calculations include vertical soil water flows in three soil layers and lateral saturated subsurface flow among pixels, evaporation from intercepted precipitation and the ground surface, transpirational loss of water from each soil layer partitioned according to active root fraction and soil water availability, accumulation and melt of snow based on air temperature, and runoff. The vertical movement within the soil profile is bi-directional and estimated through implicitly resolving equations governing the highly non-linear dependence of water diffusion on soil

moisture content (Thompson and Pollard, 1995). The methodologies for these calculations were previously introduced (Ju and Chen, 2005).

In this model, the surface runoff is simulated according to the VSMC of the first soil layer and the amount of input water (precipitation through fall and snowmelt) (Neilson, 1995). The lateral redistribution of soil water via saturated subsurface flow is simulated using a TOPMODEL-based scheme (Beven and Kirkby, 1979; Wigmosta et al., 1994). The flow rate at time t into and out of the ith pixel is computed as (Wigmosta et al., 1994)

$$q(t)_{i,j} = T(t)_{i,j} w_{i,j} \frac{e_i - e_j}{d_{i,j}}, \tag{4}$$

where $q(t)_{i,j}$ (m^3 d^{-1}) is the flow rate between pixel i to its jth neighbor; e_i and e_j are the elevations of pixels i and j (m), respectively; $w_{i,j}$ is the width of flow from i to j(m); $d_{i,j}$ is the distance between the centre of pixels i and j (m); and $T(t)_{i,j}$ is the transmissivity of soil water (m^2 d^{-1}) (Wigmosta et al., 1994) and determined by

$$T(t)_{i,j} = \begin{cases} K s_i \left(e^{-f_i z_i} - e^{-f_i D_i} \right) f_i^{-1} & \text{if } e_i > e_j \\ K s_j \left(e^{-f_j z_j} - e^{-f_j D_j} \right) f_j^{-1} & \text{else} \end{cases}, \tag{5}$$

where $K s_i$ and $K s_j$ are the lateral saturated hydraulic conductivity at the ground surface for pixels i and j (m d^{-1}); f_i and f_j are the decay rates of saturated conductivity with depth (m^{-1}); z_i and z_j are water table depths (positive downward) (m^{-1}); and D_i and D_j are the total soil depths (m).

Field measurements showed both lateral saturated hydraulic conductivity $K s$ and the decay rate of saturated hydraulic conductivity with depth f have spatial variations (Beven, 1997; Coles et al., 1997; Fraser et al., 2001). For the TOMPODEL framework, the effective $K s$ value used in the model increased with the grid size of digital elevation model (DEM) (Saulnier et al., 1997). In the current model, the $K s$ values are parameterized according to drainage class (Table 1).

Table 1. The values of surface lateral saturated hydraulic conductivity $K s$ (m d^{-1}) and the decay rate of $K s$ with depth f (m^{-1})

Drainage class[a]	$K s$ (m d^{-1})	f (m^{-1})
Very poor	10	5
Poor	15	4
Imperfect	20	3
Moderately well	25	2.5
Well	30	2
Rapid	40	1
Excessive	50	1

[a]The drainage class was defined according to that in the SLC database. The notation of drainage class: E, Excessively good; R, Rapid; G, Good; M, Moderately good; I, Imperfect; P, poor; and V, very poor.

The balance of lateral saturated subsurface flow for pixel i ($Q(t)_i$) is calculated as

$$Q(t)_i = \sum_{j=1}^{8} q(t)_{i,j}. \tag{6}$$

The monthly mean soil temperatures are calculated from air temperature with an assumption of harmonic variation of temperature with time around the annual mean (Monteith and Unsworth, 1990). The effects of LAI, litter mass and soil texture on soil temperature are considered following Paul et al. (2004).

The decomposition rates of litter and soil C pools are controlled by soil moisture content and temperature in different soil layers (Potter, 1997). The temperature and moisture of the topmost soil layer affects the decomposition of surface foliage litter and surface microbial C pools. The decomposition of other soil C pools is affected by a weighted average of decomposition modifiers of soil moisture content and temperature in the middle and lowest layers. Each layer is weighted according to the vertical distribution of active root biomass (Jackson et al., 1996) and the drainage class. In poorly drained areas, the lower layer is assigned a higher weight; field measurements have shown that, in poorly drained boreal areas, soil organic C content at depth have very low decomposition rates (Trumbore and Harden, 1997; Rapalee et al., 1998).

The updated InTEC model (V3.0) uses different methods to initialize the various C pools for forests and wetlands. For forests, the initialization assumes that C dynamics were in steady state (i.e. inputs equal to outputs) prior to 1901 (for stands disturbed after 1901) or in the year before the last fire disturbance (for stands undisturbed after 1901) (Chen et al., 2003). The C content was initialized using the average climatology from 1901 to 1910. The initialization was run until C dynamics reached a quasi steady state, when the absolute value of NEP became smaller than 2% of NPP. In the simulation, a stand-replacing forest disturbance was forced to occur at a 250-yr interval, which is roughly equivalent to the mean age of natural mortality and the average fire return period of boreal forests (White et al., 2000). For wetlands, the initialization assumed a steady-state C balance for 'fast' C pools but not 'slow' C pools. Studies have shown that northern wetlands have been persistent C sinks over the past 5000–1000 yr (Tolonen et al., 1992; Gorham, 1995; Turunen et al., 2002). We applied the steady-state assumption, identical to the forest initilization, to the four biomass pools (foliage, stem, fine root and coarse root), five litter pools (surface structural, surface metabolic, soil structural, soil metabolic, and woody), and two microbial pools (surface microbial and soil microbial). The initial sizes of these pools were determined by solving a set of differential equations that describe their C balances. In contrast, the slow and passive soil C pools were allowed to continuously increase (Rapalee et al., 1998; Frolking et al., 2001) and their initial values were set following Frolking et al. (2001, 2002)

using an integration period of 100 yr for the slow C pool and 8000 yr for the passive C pool.

Errors in the initialized C pools are a major source of uncertainties in modelled estimates of the current C balance. However, it is impossible to trace the historical C dynamics for each pixel due to the shortage of historical climatic, vegetation and soil C inventory data. Our assumption of steady-state C dynamics prior to disturbance is imperfect but, unlike other schemes, it does attempt to make use of disturbance history where available. Other initialization schemes exist, but each has weaknesses. Total soil C may be allocated into various C pools using prescribed coefficients (Potter et al., 1993). More commonly, the C pools are initialized by running the model for many years using mean climate, N deposition and stand age. The model is run until the C pools reach a near steady state, representing the state of the ecosystem before industrialization (White et al., 2000). Using the SLC data set to constrain the model, systematic errors in initializing C content are greatly reduced, and after 98 yr of simulation, the effect of the remaining errors on the current C flux estimation is reduced by a factor of eight (Chen et al., 2003).

3. Data used

A variety of data sets, including remote sensing, climate, soil texture, N deposition, and DEM, were produced and compiled from various sources to drive the model. Before or during the model execution, all spatial data sets at 1 km resolution were processed into a standard Lambert conformal conic (LCC) projection with $49°$ and $77°$ N standard parallels and a 95 °W meridian.

3.1. Remote sensing data

Remote-sensing data from AVHRR and VEGETATION were used to produce Canada-wide maps of LAI in 1994 (Chen et al., 2002), land cover in 1994 (Cihlar et al., 1998) and forest stand age in 1998 (Chen et al., 2003). There are 31 cover types in the land cover map, of which type 1 to type 15 are forest cover types, including upland forests and wetlands. All of these 15 types are included in the simulation and grouped into four classes, each of which is specifically parameterized (Chen et al., 2003). Remotely sensed data from the VEGETATION sensor on the board of the SPOT 4 satellite were used in conjunction with the Canadian large-fire data base and forest inventory data to construct a map of forest stand age in 1998, a key input for estimating the pixel-based C budget (Amiro and Chen, 2003; Chen et al., 2003).

3.2. Climate data

Monthly mean air temperature and precipitation for Canada for the period 1901–1998 were obtained from the 0.5° global data set interpolated by the UK Climate Research Unit from available station observations using the methods of (New et al., 1999, 2000). The monthly temperature data were averaged to obtain spring (March–May), growing season (June–August) and annual mean temperatures. The precipitation, temperature and water vapour pressure in 0.5° grid cells were interpolated to 1-km resolution using a bilinear interpolation scheme without the consideration of topographic effects (Liu et al., 1999). The monthly temperature range, water vapour pressure and precipitation were linearly interpolated into quasi-daily values for estimating global solar irradiance following Thornton and Running (1999). From estimated daily values, monthly solar irradiance for each pixel was produced.

3.3. Nitrogen deposition data

N deposition is an important supply of N to boreal forests. N deposition may both accelerate the expansion and the productivity of forests. Kochy and Wilson (2001) found that available soil N increased significantly with N deposition in the northern Great Plains of Canada. A statistically significant positive relationship was found between N deposition alone and present-day C accumulation in both hummocks and hollows of ombrotrophic peatlands in eastern Canada (Turunen et al., 2004). N deposition data for Canada's forests during 1983–1994 obtained from measurements made by the Canadian Air and Precipitation Monitoring Network (CAPMoN) (Ro et al., 1995) were spatially interpolated and extrapolated to produce a N deposition map in Canada. The annual N deposition value of each pixel in this map was temporally extrapolated for the 1901–1982 period based on historical greenhouse gas emission in Canada (Chen et al., 2003).

3.4. Soil landscape of Canada database

Data sets including soil texture (sand, silt and clay fractions), drainage class, and soil organic C mass per unit area were compiled from the SLC database consisting of about 15 000 polygons, which is the best soil database currently available for Canada (Schut et al., 1994; Lacelle, 1998; Tarnocai, 1998). Soil texture was used to determine hydrological parameters, including porosity, field capacity (water potential at 33 kPa), wilting point (water potential at 1500 kPa), saturated hydraulic conductivity, and air entry water potential (Saxton et al., 1986; Campbell and Norman, 1998). The hydraulic properties of peatlands were parameterized following Letts et al. (2000) and Fraser et al. (2001). The soil C content of a polygon was computed as a weighted mean of the sub-regions, where each sub-region was weighted by its area fraction. The soil C content of each sub-region was the product of soil horizon depth, soil bulk density and the ratio of organic C, which are in the attribute table of the SLC database. To generate these data layers with the same projection and resolution as other data layers, the original vector data of SLC were merged, reprojected, and rasterized using the ARC/INFO geographic information system.

3.5. Digital elevation model data

The DEM data used here is the product of Canada 3D provided by the Canadian Forest Service, Ontario region. This data set was derived from the cells of the Canadian Digital Elevation Data at a 1:250,000 scale. This data set is recorded in ASCII format and available in two resolutions: grids regularly spaced at 30 or 300 arcsec. The elevation values are expressed in meters with respect to the mean sea level, in accordance with the North American Datum of 1983 (NAD83). Since the 30 arcsec data set has a better spatial resolution (about 580 m) than the 300 arcsec data set, it was registered and re-projected to derive the wetness index map and to calculate local slopes for simulating the horizontal redistribution of soil water.

3.6. Tower-flux data

Multi-year net fluxes of CO_2, measured using the eddy-covariance method at four forest sites and one peatland site, were used for model validation. The fluxes had been corrected for the underestimation of respiratory fluxes on calm nights (Barr et al., 2004). Three of the forest sites are located in the BOREAS SSA/BERMS study area, including a 73-yr-old aspen site (SOA) (53.628°N, 106.198 °W) (Black et al., 1996; Barr et al., 2004), a 121-yr-old black spruce site (SOBS) (53.987°N, 105.118°W) (Jarvis et al., 1997; Arain et al., 2002), and a 65 yr-old jack pine site (SOJP) (53.916°N, 104.692°W) (Griffis et al., 2003). The fourth forest site is a 53-yr-old Douglas-fir forest (DF) (49.850°N, 125.317°W) on Vancouver Island, BC (Humphreys et al., 2003). The peatland site, MB (Mer Bleue), is an ombrotrophic bog East of Ottawa, Ontario, Canada (45.40°N, 75.50°W) (Lafleur et al., 2003). Monthly means of VSMC measured in the growing season (May–October) at the four forest sites and the year-round water table depth observed at SOBS and MB during 1998–2002 were used to validate the hydrological module.

4. Results and discussion

4.1. Relationship between drainage class and soil carbon content

To test the hypothesis that drainage is one of the major determinants of local soil organic C accumulation, the linkage between soil C content and drainage class was statistically analysed using data compiled from the SLC database. The analysis was based on 10 040 sub-regions from the database with the soil C content measured at sampling sites, excluding sub-regions where the soil C content was not measured directly. Generally, the total soil organic C content is related to the drainage class, with the largest C content occurring in very poorly drained regions (Fig. 1). The mean soil C content increased exponentially from 10.8 kg C m^{-2} in excessively well-drained regions to 175 kg C
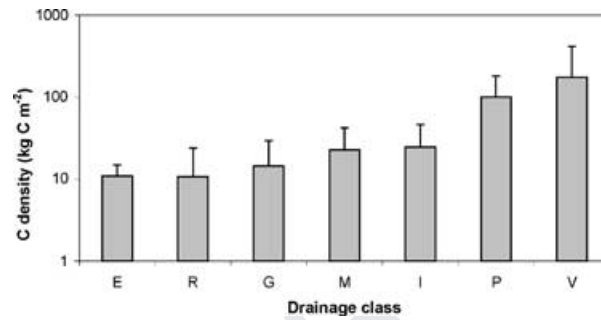

Fig 1. The dependence of soil C stocks on drainage conditions. The error bar represents a standard deviation of soil C stocks for each drainage class. The y-axis is in logarithmic scale.

m^{-2} in very poorly drained regions. The soil C content was significantly higher in poorly or very poorly drained regions than in regions with good drainage conditions. In more than 67% of the very poorly drained regions, the soil C content was above 100 kg C m^{-2}, over 10 times higher than that in excessively or rapidly well-drained areas. This overall dependence of soil C on drainage class is very similar to the observations of Rapalee et al. (1998) in the BOREAS Northern Study Area (NSA), where the total soil C content ranged from 3.6 kg C m^{-2} in well-drained jack pine stands to 144 kg C m^{-2} in very poorly drained bogs. The variability of soil C content within each drainage class was also related to drainage conditions. Soil C content had the highest variability in very poorly drained regions, with a standard deviation of 244 kg C m^{-2}, and the lowest variability in excessively well-drained regions, with a standard deviation of only 4 kg C m^{-2}. The large variability of soil C content in very poorly drained regions suggests that, although drainage is the dominant controller of soil C content, other factors such as climate, stand age, and land cover type also have significant influences on soil C accumulation.

4.2. Modelled soil moisture content and water table depth compared with measurements

Soil moisture content is a critical factor in the terrestrial C balance. The decomposition of soil organic C decreases exponentially with the departure of soil moisture content from the optimum value for microbial activities, typically about 60% of the porosity (Potter, 1997; Frolking et al., 2002). A small error in the simulation of soil moisture content can cause significant errors in estimated heterotrophic respiration and consequently the C budget. We tested the ability of InTEC V3.0's hydrological module to simulate seasonal variations of soil moisture content in the surface layers, based on growing-season (May–October) monthly mean VSMC measured at the four forested flux-tower sites during 1998–2002. The drainage class is rapid at SOJP and poor at SOBS. The SOA and DF sites are moderately well drained. Simulations were compared with observations for
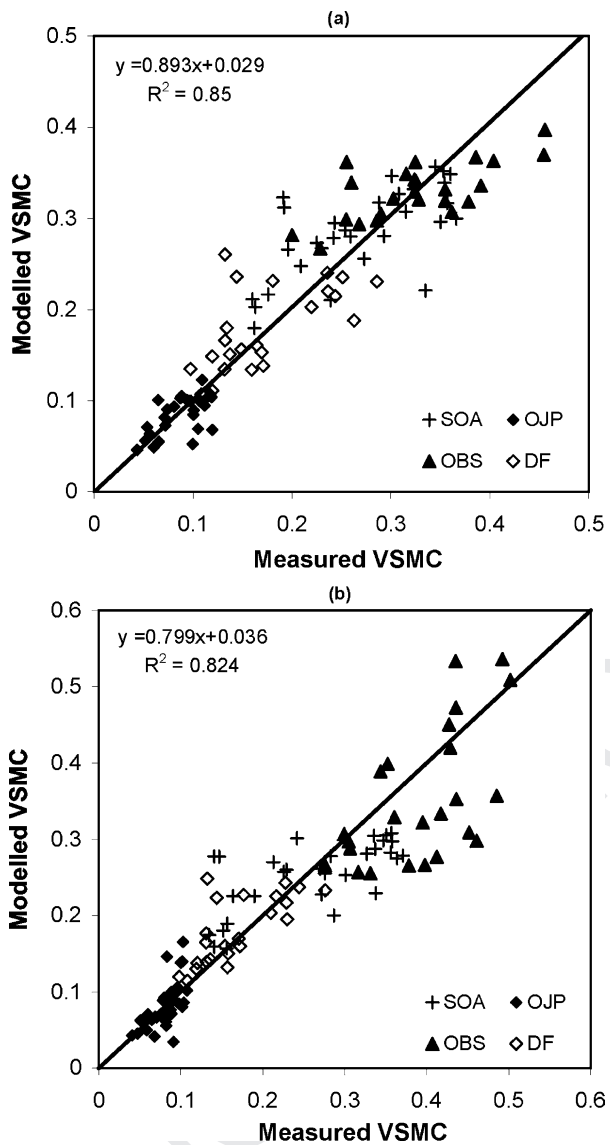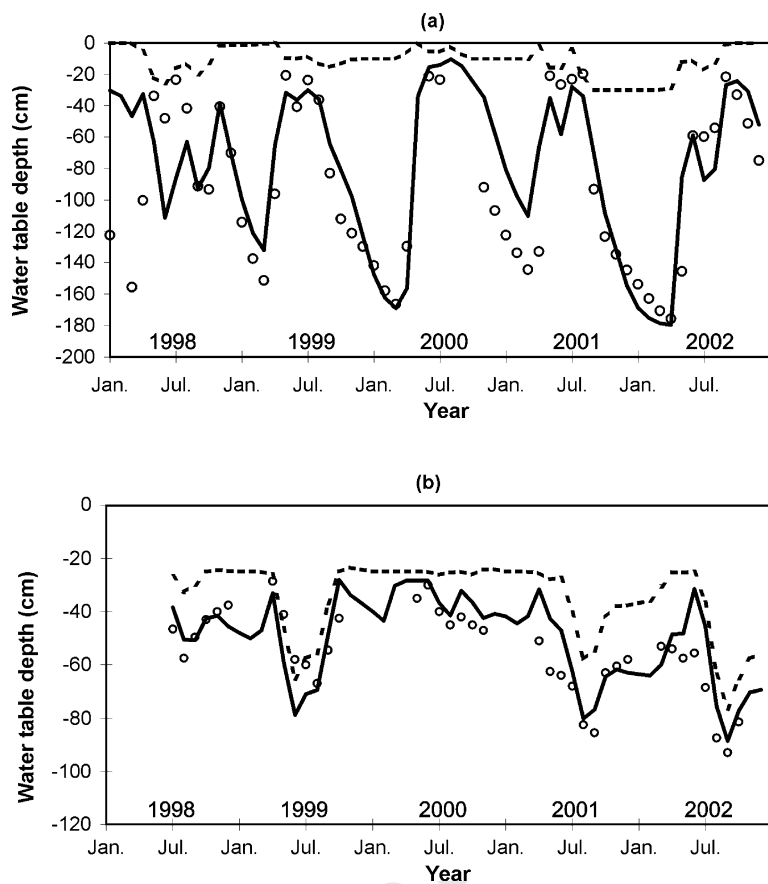
Fig 2. Comparison of modelled monthly mean volumetric soil moisture content (VSMC) with measurements in the growing season (May to October) at four tower-flux sites: (a) 0–10 cm; (b) 10–30 cm. All measurements of VSMC were interpolated or extrapolated and then averaged to values in the 0–10 cm and 10–30 cm depths. SOA: 75-yr-old aspen site, Saskatchewan; SOBS: 121-yr-old black spruce site, Saskatchewan; SOJP: 65-yr-old jack pine site, Saskatchewan; and DF: 53-yr-old Douglas-fir site, Vancouver Island, BC. The straight solid line is the 1:1 line.

0–10 cm and 10–30 cm depths (Fig. 2). The model captured 85% (0–10 cm) and 82% (10–30 cm) of the variability of VSMC in the growing season across these forested sites. However, the model underestimated VSMC of the 10–30 cm layer during wet months at SOA. At SOBS, it tended to underestimate VSMC for the 0–10 cm layer in wet months and for the 10–30 cm layer in

moderately wet months. In dry times, the simulated VSMC of the 0–10 cm layer was higher than measurements.

Water table depth is an important factor determining the net C exchange of wetlands because it changes the relative importance of aerobic and anaerobic processes (Lafleur et al., 2003; Humphreys et al., 2004). In non-wetland areas, water table depth is critical for estimating soil moisture content. The current model calculates water table depth based on the relative saturation of each soil layer (Letts et al., 2000). To investigate the importance of including lateral saturated subsurface flow for the simulation of water table depth, the model was run under two scenarios, with and without lateral saturated subsurface flow. The modelled monthly mean water table depth was compared with observations at the SOBS and MB sites (Fig. 3). The SOBS site is dominated by black spruce (*Picea mariana*) and has generally flat topography, with local slopes smaller than 1%. This area contains abundant wetland areas and the drainage condition is poor. The water table is normally near the surface during the growing season because the area is poorly drained and precipitation and snowmelt often exceed evapotranspiration. After September, the slow drainage of soil water and upward vapour diffusion to the freezing front causes a decrease in water table depth to about 1.5 m below the surface. The simulation that included lateral subsurface flow was able to capture the seasonality of the water table depth. Without lateral subsurface flow, the model failed to predict the seasonal variability in water table depth; in particular, the modelled water table was too shallow in non-growing seasons. The MB site is a 28 km^2 ombrotrophic bog characterized by several raised peat domes. Its current elevation is from 67 to 70 m. Peat depths range from 2.0 m at the edges to more than 5.0 m in the centre and are underlain by Champlain Sea marine clays. Estimated horizontal hydraulic conductivity K_h in the upper peat layer ($\sim$0–0.45 m) decays in magnitude from the peat surface, ranging from 10^{-7} to 10^{-3} m s^{-1}. K_h estimates for the lower peat depths range from 10^{-8} to 10^{-6} m s^{-1} (Fraser et al., 2001). The bog surface around the tower site has a hummock-hollow microtopography, with a mean relief between hummock tops and the hollow bottoms of 0.25 m. Hummocks compose 70% of the surface and have a median diameter of about 1.0 m. The water table is usually at or below the bottom of the hollows (Lafleur et al., 2003). Water table depth can vary considerably within the growing season (Fig. 3). The interannual variability of water table depth at this site is also notable. The water table was higher in 2000 than in other years due to above normal precipitation and cool temperature. The water table tended to become deeper after the fall of 2000 owing to a decrease in precipitation. The summer of 2001 was drier than normal, with 105 mm precipitation (only 41% of the long-term mean). By the end of this summer, the water table was about 30 cm lower than in 2000. The inclusion of lateral subsurface flow significantly improved the agreement between model simulations and observations of water table depth whereas, without lateral subsurface flow, the simulated water table depth was mostly shallower than the

Fig 3. Comparison of modelled monthly mean water table depth with measurements at (a) Southern Old Black Spruce, and (b) Mer Bleue peatland site. Dots represent measured monthly mean water table depth. Solid and dash lines are modelled water depth with and without lateral saturated base flow, respectively. For the Mer Bleue site, the measured water table depth presented here is the average of measurements taken at two wells, located at a hummock and a hallow about 1.2 m apart. For the Southern Old Black Spruce site, water table depth is taken at one well.

measurements. The improvement in the simulation of water table depth reduced the discrepancy between simulated and observed NEP. The root-mean-square-error (RMSE) value of simulated NEP was reduced from 37 to 31 g C m^{-2} yr^{-1} ($n = 4$) for MB (the mean of measured NEP in 4 yr was 46 g C m^{-2} yr^{-1}) and from 46 to 41 g C m^{-2} yr^{-1} ($n = 7$) (the average of measured NEP in 7 yr was 37 g C m^{-2} yr^{-1}) for SOBS. The model simulations demonstrate that lateral subsurface flow is an important hydrologic process that must be included in coupled C cycle-hydrologic models.

The InTec V3.0 model was able to reproduce the main features in the seasonal cycles of soil moisture content and water table depth at contrasting sites. The occasional departure of modelled soil moisture content and water table depth from the measurements can be attributed to following factors. First, the spatial and temporal resolutions of the model are relatively coarse. The model's use of a monthly time step leads to errors in the partitioning of precipitation into intercepted water, surface runoff, and infiltration, and in the estimation of vertical percolation. The use of a 1 km resolution leads to errors in lateral flow associated with the impact of local microtopographic variations at small spatial scales, such as hummocks and hollows. Second, the scheme that is used to estimate soil hydraulic parameters may be

overly simplistic. All hydraulic parameters are estimated from soil texture or drainage class using literature-based empirical equations or values. All are treated to be vertically uniform except for saturated hydraulic conductivity, which is assumed to decline exponentially with depth from the surface. Considering the vertical and horizontal heterogeneity of soil properties and the demonstrated importance of vertical and lateral water flow, more detailed parameterizations of soil hydraulic properties are needed to reduce the uncertainties in simulated soil moisture content and water table depth. Further, in this model, the redistribution of soil water is driven by surface topography and water table depth mirrors local topography. Recent studies show that this assumption could overestimate the effects of topography on runoff and lateral saturated subsurface flow in areas such as the sub-humid glaciated Boreal Plain of western Canada, where climate, bedrock geology, surficial geology, soil type and depth play more important roles in soil water redistribution than does topography (Devito et al., 2005a,b). The roles of bedrock and surficial geology are not included in current simulations, possibly giving rise to some uncertainties in simulated soil moisture and water table depth in areas with uneven bedrocks, coarse deposits, and complex interactions between surface water and groundwater.

4.3. Validation of modelled net ecosystem productivity with tower-flux data

The model estimates of NEP were validated using eddy-covariance measurements from five tower-flux sites. The simulations used climate data from the flux towers for the most recent years and spatially interpolated historical monthly climate data prior to the tower data. The NEP validation showed generally good agreement between simulated and measured values (Fig. 4). Simulations that excluded lateral flow explained 72% of the interannual variability in NEP at the five flux towers. When lateral flow was included, the agreement improved, with the model explaining 84% of the interannual variability in NEP. However, the InTEC model at times underestimated the measured NEP extremes. The largest NEP values occurred at the Douglas-fir stand on Vancouver Island, BC, which was a large C sink. Measured annual NEP during 1997–2001 ranged from 270 to $420 \, \mathrm{g \, C \, m^{-2} \, yr^{-1}}$. Although modelled and measured NEP had similar ranges, the model predicted smaller values of C sink than the observations for all years except 1998. This underestimation may be due to an aerial application of N fertilizer of $200 \, \mathrm{g \, N \, m^{-2}}$ at the DF site in 1995, which was not accounted for in the model and may have significantly increased NEP (Chen et al., 2003). For the 73-yr-old BOREAS/BERMS old aspen stand, modelled NEP agreed with measurements in most years but was much smaller than the measurement in 2001. In this year, the measured NEP value of $367 \, \mathrm{g \, C \, m^{-2} \, yr^{-1}}$ was much higher than normal (the mean of measured NEP from 1994 to 2002 is 171 g C m^{-2} yr^{-1}) due to an early start of photosynthesis (Barr et al.,

2004) and low heterotrophic respiration (Kljun et al., 2004). The model predicted an above normal NEP value ($241 \, \mathrm{g \, C \, m^{-2} \, yr^{-1}}$) in this year but failed to predict the magnitude of increase in annual NEP, presumably because the model's annual time step was too coarse to fully capture the critical importance of interannual differences in growing-season length and heterotrophic respiration and soil moisture content. At the 65-yr upland SOJP site, the model slightly overestimated NEP. For the Mer Bleue wetland and the 121-yr-old SOBS site, the modelled annual NEP values mirrored the tower data well.

The new hydrological components in InTEC V3.0 significantly improved the model's ability to simulate the interannual variability in NEP at flux-tower sites. Further improvements may be achieved by using a finer time step. Although the first-order interannual variability of climate has been considered through the use of spring and growing-season temperatures, the annual time step used for the NPP calculation may be too large to fully capture interannual variability of photosynthesis and respiration. In addition, current model is unable to describe the strong non-linearities between soil moisture or temperature and corresponding heterotrophic respiration using simulated monthly soil moisture and temperature to evaluate abiotic controls on decomposition processes. A finer temporal model resolution or a temporal scaling up scheme would remedy this problem but would require more frequent climate data and more computation resources.

4.4. Effect of drainage class on errors of modelled soil carbon content

The total soil C, including detritus and soil organic C, was simulated pixel-by-pixel based on modelled historical annual NPP values, vegetation turnover rates to detritus, decomposition rates of all C pools, and fire disturbance. The simulated soil C content was compared with that compiled from the SLC database at the polygon scale. Of the ~15 000 polygons in the SLC database, 2228 were selected for model validation, based on the criterion that the areal sum of sub-regions with soil C measurements account for at least 50% of the area of the polygon.

InTEC V3.0 captured the spatial distribution of soil C content among various drainage and climatic conditions. It significantly reduced the underestimation of soil C content by InTEC V2.0 (Ju and Chen, 2005). To investigate the sensitivity of errors in modelled soil C to drainage class, the modelled polygon-mean soil C content from versions 2.0 and 3.0 of InTEC was compared with the SLC data for each drainage class (Fig. 5). Similar to soil C, the drainage class of each polygon was compiled from the SLC database as the area-weighted mean of drainage classes of all sub-regions in a polygon. The mean bias error (MBE) and RMSE were employed as criteria for the sensitivity analysis. For both versions of InTEC, the magnitudes of MBE and RMSE generally decreased from very poor to excellent drainage class. Version 3.0 outperformed version 2.0 in the estimation of soil C in very poorly, poorly, imperfectly and moderately well-drained
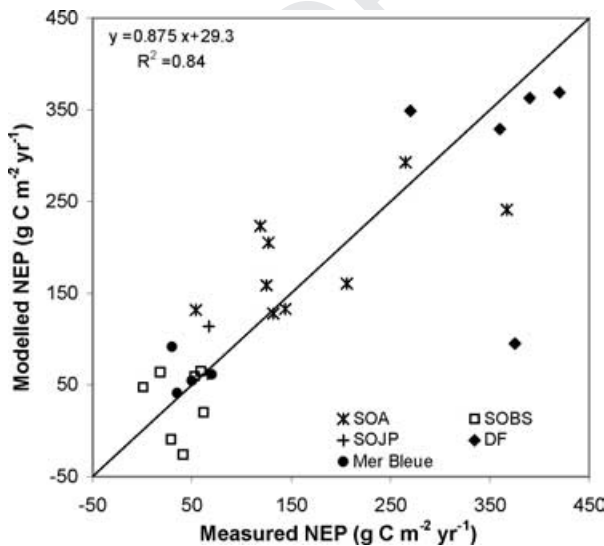

Fig 4. Modelled annual NEP compared with eddy-covariance measurements at four forest sites and a peatland site. SOA: Old aspen stand in the SSA of BOREAS; SOBS: Old black spruce stand in the SSA of BOREAS; SOJP: Old jack pine stand in the SSA of BOREAS; DF: Doglas-fir stand in Vancouver Island, BC; MB: Mer Bleue peatland site, Ottawa, ON. The straight solid line is the 1:1 line.
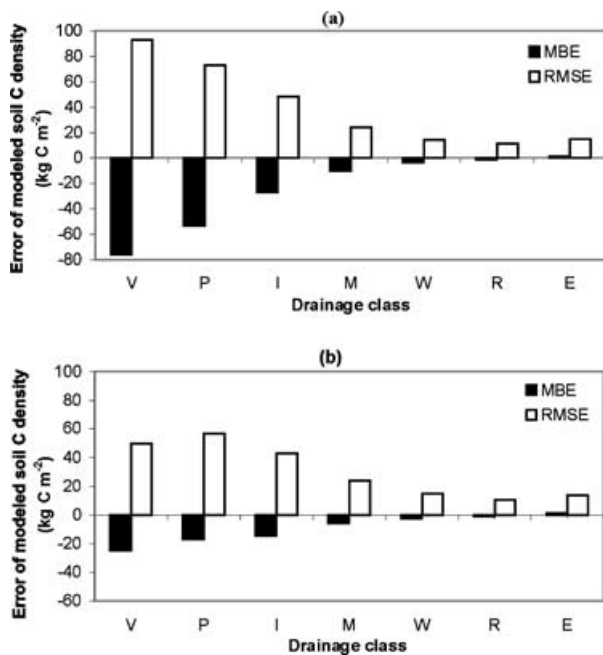
Fig 5. The sensitivity of errors in modelled soil C density to drainage conditions. The modelled polygon-mean soil density was compared with the value in SLC. The root mean square error (RMSE) and the mean bias error (MBE) are computed as: $\text{RMSE} = \sqrt{\frac{\sum (C_{\text{SLC}} - \hat{C})^2}{N}}$, $\text{MBE} = \frac{\sum (\hat{C} - C_{\text{SLC}})}{N}$, where C_{SLC} is the mean soil C density within a polygon of SLC database file (kg C m^{-2}), $\hat{C}$ is the simulated mean soil C density (kg C m^{-2}), and N is the number of polygons in each drainage class. The notation of drainage classes is the same as in Fig. 1. (a) from InTEC V2.0; (b) from InTEC V3.0.

areas. Both versions of InTEC were able to estimate soil C content in areas with good, rapid and excessive drainage, with a slight underestimation in well and rapidly drained locations and a slight overestimation in excellently drained locations. We conclude that: (1) errors of simulated soil C content are sensitive to drainage conditions and (2) the simulation of soil C content under various terrain conditions requires a robust description of

the hydrological cycle, with lateral flow and separate parameterizations for forests and wetlands.

4.5. *Effect of hydrology on the estimation of regional carbon balance*

Canada-wide C balances in forests and wetlands, simulated by the two versions of the pixel-based InTEC model, were compared to evaluate the degree to which the estimation of regional C balances depend on the inclusion of detailed drainage information in the model. The comparison is summarized in Figs 6 and 7. Overall, InTEC V2.0 and V3.0 produced very similar temporal trends of C balances for 20th century. Both versions showed three distinct temporal phases, driven by disturbance history. Large disturbances during the late–19th-century and the first decade of the 20th century caused Canada's forests and wetlands together to be a small C source at the beginning of the 20th century. Subsequent forest regeneration, accompanied by the positive effects of climate and atmospheric changes, shifted Canada's forests and wetlands from a C source to a C sink, with peak C uptake in the middle of the 20th century. In the late–20th-century, an increase in fire disturbance frequency and a shift in the forest age-class structure caused a gradual decline in the C sink strength, although the positive effects of climatic and atmospheric changes were still significant (Fig. 6). However, the two InTEC model versions differed in long-term C accumulation and interannual variability. The mean national C sink simulated by V3.0 for 1901–1998 was 111.9 Tg C yr^{-1}, which is 41.4 Tg C yr^{-1} higher than the value of 70.5 Tg C yr^{-1} simulated by V2.0. V3.0 also simulated greater interannual variability than V2.0. Spatially, the increase of C sinks from V2.0 to V3.0 occurred mainly in wetland regions (Fig. 7). For example, the sink strength in the wetlands near Hudson Bay increased from 10 to 20 g C m^{-2} yr^{-1}. The wetlands in the Mackenzie Valley shifted from small C sources to small C sinks. For upland forests, where the most significant control on the C balance is stand age (Rapalee et al., 1998; Chen et al., 2003), the two models produced similar C balances.
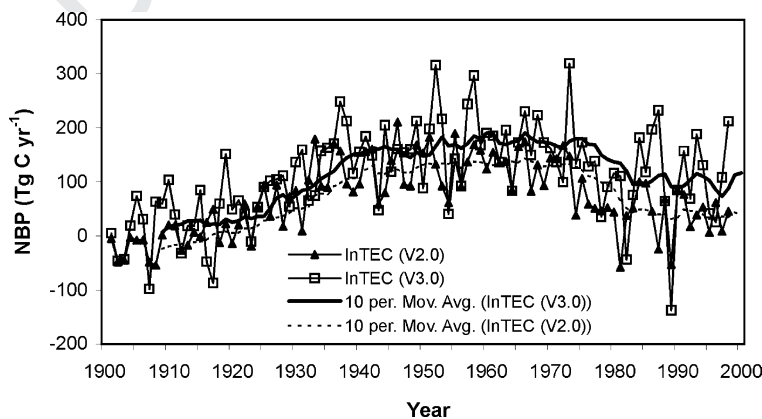

Fig 6. Carbon balance of Canada's forests and wetlands over the last century simulated using versions 2.0 and 3.0 of the InTEC model. InTEC (V2.0) includes forests only, while InTEC (V3.0) includes both forests and wetlands with a new hydrologic module to consider the subsurface baseflow and a different parameterization scheme for wetlands.
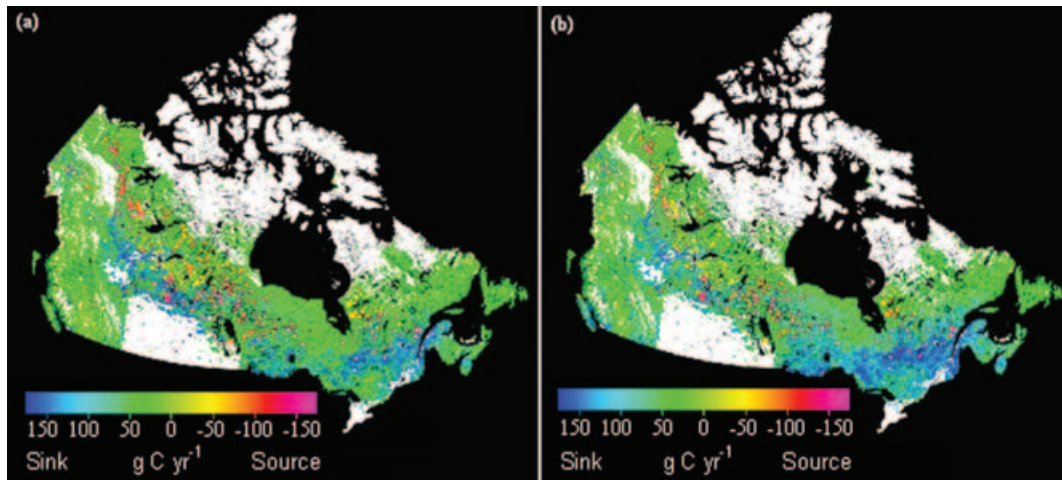
Fig 7. Comparison of simulated carbon source and sink distributions in Canada's forests and wetlands averaged for the period 1990–1998. (a) from InTEC V2.0; (b) from InTEC V3.0.

The differences between the two model versions are related to differences in two assumptions. First, whereas V2.0 assumed that the wetland C cycle was in steady state during the pre-industrial period, V3.0 more correctly assumed that wetlands are a small but persistent C sink (Gorham, 1995; Frolking et al., 1998; Rapalee et al., 1998; Waddington et al., 1998). The change in wetland soil C initialization between V2.0 and V3.0 resulted in an increased C sink for all pixels of wetlands (mostly forested wetlands). The method to initialize C content has a considerable impact on the simulated C balances. The use of forest inventory and the SLC database for biomass and soil C validation may, to some degree, minimize errors caused in the initialization scheme. Second, whereas V2.0 estimated the annual abiotic decomposition modifier at an annual time step, based on simulated annual mean soil temperature and moisture, V3.0 estimated the modifier as the mean of monthly estimates, based on simulated monthly mean soil temperature and soil moisture content. This change caused a much greater expression of interannual climatic effects on heteorotrophic respiration in V3.0 than in V2.0.

5. Conclusions

The impact of hydrology on soil C accumulation was investigated through simulating soil C content and analysing the variability of soil C content as a function of drainage class. The pixel-based InTEC model V2.0 was improved by separating the parameterizations for forests and wetlands and incorporating a process-based hydrological module, which simulates the spatial and temporal dynamics of soil temperature and moisture content within three soil layers using spatially distributed climate, vegetation, soil, DEM and drainage class data sets. This three-dimensional hydrological module includes topographic effects on the spatial redistribution of soil water. The hydrologic

module was able to capture major seasonal and interannual variability in soil moisture content and water table depth at five sites within the Fluxnet-Canada Research Network. Compared with the earlier version of InTEC (V2.0), which lacked these modifications, the new InTEC model (V3.0) considerably improved the agreement of simulated annual NEP and soil C content with field measurements. This study led to three principal conclusions:

(1) Soil C accumulation depends primarily on drainage class. Nationally, the average soil C mass per unit area increased exponentially from 10.8 kg C m^{-2} in excessively well-drained regions to 175 kg C m^{-2} in very poorly drained regions. Within each drainage class, soil C accumulation was more variable in poorly drained regions than in regions with rapid drainage. These results demonstrate the importance and difficulty of simulating soil C content and ecosystem C balances for poorly drained regions.

(2) Topography and drainage class both play important roles in the redistribution of soil water. In order to successfully simulate soil moisture content and water table depth for reliable estimates of the C balance, lateral water flow should be included in regional terrestrial C models. Three additional changes to the hydrologic module may further improve model performance: adding a parameterization scheme that considers the vertical heterogeneity of soil properties, including the effects of bedrock and surficial geology and those of local micro-topography at spatial scales smaller than the current 1-km resolution on soil water redistribution, and integrating interactions of surface water and groundwater in the hydrological module.

(3) Poorly drained regions, mainly wetlands, contribute significantly to C sinks in Canadian forests and wetlands. The addition of a separate parameterization for wetlands and the inclusion of a process-based hydrological module in InTEC (V3.0) increased our estimate of the average Canadian forest-wetland C sink for 1901 to 1998 from 70.5 Tg C yr^{-1} (InTEC V2.0) to

111.9 Tg C yr^{-1} (InTEC V3.0). The increase occurred mainly in poorly drained areas. The significant difference in simulated C balance from these two versions of InTEC encourages further efforts on detailed hydrological representation and wetland parameterization in estimating regional C budgets.

6. Acknowledgments

References

Alm, J., Schulman, L., Walden, J., Nykanen, H., Martikainen, P. J. and Silvola, J. 1999. Carbon balance of a boreal bog during a year with an exceptionally dry summer. *Ecology* **80**, 161–174.

Amiro, B. D. and Chen, J. M. 2003. Forest-fire-scar aging using spot-vegetation for Canadian ecoregions. *Canadian Journal of Forest Research* **33**, 1116–1125.

Arain, M. A., Black, T. A., Barr, A. G., Jarvis, P. G., Massheder, J. M., Verseghy, D. L. and Nesic, Z. 2002. Effects of seasonal and interannual climate variability on net ecosystem productivity of boreal deciduous and conifer forests. *Canadian Journal of Forest Research* **32**, 878–891.

Ball, J. T., Woodrow, I. E. and Berry, J. A. 1987. A model predicting stomatal conductnance amd its contribution to the control of photosynthesis under different environmental conditions. In: *Progress in Photosynthesis Research* (ed. J. Biggins). Martinus Nijhoff Publishers, Dordrecht, 221–224.

Baron, J. S., Hartman, M. D., Band, L. E. and Lammers, R. B. 2000. Sensitivity of a high-elevation rocky mountain watershed to altered climate and co2. *Water Resources Research* **36**, 89–99.

Barr, A. G., Black, T. A., Hogg, E. H., Kljun, N., Morgenstern, K. and Nesic, Z. 2004. Inter-annual variability in the leaf area index of a boreal aspen-hazelnut forest in relation to net ecosystem production. *Agricultural and Forest Meteorology* **126**, 237–255.

Beven, K. 1997. TOPMODEL: a critique. *Hydrological Processes* **11**, 1069–1085.

Beven, K. J. and Kirkby, M. J. 1979. A physically based variable contributing model of basin hydrology. *Hydrological Science Bulletin* **24**, 43–69.

Black, T. A., Denhartog, G., Neumann, H. H., Blanken, P. D., Yang, P. C., Russell, C., Nesic, Z., Lee, X., Chen, S. G., Staebler, R. and Novak, M. D. 1996. Annual cycles of water vapour and carbon dioxide fluxes in and above a boreal aspen forest. *Global Change Biology* **2**, 219–229.

Blanken, P. D. and Black, T. A. 2004. The canopy conductance of a boreal aspen forest, prince albert national park, Canada. *Hydrological Processes* **18**, 1561–1578.

Bonan, G. B., Levis, S., Sitch, S., Vertenstein, M. and Oleson, K. W. 2003. A dynamic global vegetation model for use with climate models: concepts and description of simulated vegetation dynamics. *Global Change Biology* **9**, 1543–1566.

Campbell, G. S. and Norman, J. M. 1998. *An Introduction to Environmental Biophysics*. Springer-Verlag, New York, 129–144.

Chen, W. J., Black, T. A., Yang, P. C., Barr, A. G., Neumann, H. H., Nesic, Z., Blanken, P. D., Novak, M. D., Eley, J., Ketler, R. J. and Cuenca, A. 1999a. Effects of climatic variability on the annual carbon sequestration by a boreal aspen forest. *Global Change Biology* **5**, 41–53.

Chen, J. M., Liu, J., Cihlar, J. and Goulden, M. L. 1999b. Daily canopy photosynthesis model through temporal and spatial scaling for remote sensing applications. *Ecological Modelling* **124**, 99–119.

Chen, W. J., Chen, J. and Cihlar, J. 2000a. An integrated terrestrial ecosystem carbon-budget model based on changes in disturbance, climate, and atmospheric chemistry. *Ecological Modelling* **135**, 55–79.

Chen, W. J., Chen, J., Liu, J. and Cihlar, J. 2000b. Approaches for reducing uncertainties in regional forest carbon balance. *Global Biogeochemical Cycles* **14**, 827–838.

Chen, J. M., Pavlic, G., Brown, L., Cihlar, J., Leblanc, S. G., White, H. P., Hall, R. J., Peddle, D. R., King, D. J., Trofymow, J. A., Swift, E., Van Der Sanden, J. and Pellikka, P. K.E. 2002. Derivation and validation of Canada-wide coarse-resolution leaf area index maps using high-resolution satellite imagery and ground measurements. *Remote Sensing of Environment* **80**, 165–184.

Chen, J. M., Ju, W. M., Cihlar, J., Price, D., Liu, J., Chen, W. J., Pan, J. J., Black, A. and Barr, A. 2003. Spatial distribution of carbon sources and sinks in canada's forests. *Tellus B* **55**, 622–641.

Chen, J. M., Chen, X. Y., Ju, W. M. and Geng, X. Y. 2005. Distributed hydrological model for mapping evapotranspiration using remote sensing inputs. *Journal of Hydrology* **305**, 15–39.

Cihlar, J., Xia, Q. H., Chen, J., Beaubien, J., Fung, K. and Latifovic, R. 1998. Classification by progressive generalization: a new automated methodology for remote sensing multichannel data. *International Journal of Remote Sensing* **19**, 2685–2704.

Coles, N. A., Sivapalan, M., Larsen, J. E., Linnet, P. E. and Fahrner, C. K. 1997. Modelling runoff generation on small agricultural catchments: can real world runoff responses be captured? *Hydrological Processes* **11**, 111–136.

Devito, K. J., Greed, I. F. and Fraser. 2005a. Controls on runoff from a partially harvested apsen-forested headwater catchment, Boreal Plain, Canada. *Hydrological Processes* **19**, 3–25.

Devito, K. J., Greed, I., Gan, T., Mendoza, C., Petrone, R., Silins, U. and Smerdon, B. 2005b. A framework for broad-scale classification of hydrologic response units on the Boreal Plain: id topography the last thing to consider? *Hydrological Processes* **19**, 1705–1714.

D'odorico, P., Laio, F., Porporato, A. and Rodriguez-Iturbe, I. 2003. Hydrologic controls on soil carbon and nitrogen cycles. II. A case study. *Advances in Water Resources* **26**, 59–70.

Dickinson, R. E., Sellers, A. H., Kennedy, P. J. and Wilson, M. F. 1986. Biosphere-atmosphere transfer scheme (BATS) for the NCAR community climate model. NCAR Tech. Note TN-275, National Center for Atmosphere Research, Boulder, Colorado, USA.

Farquhar, G. D., Caemmerer, S. V. and Berry, J. A. 1980. A biochemical-model of photosynthetic CO_2 assimilation in leaves of c-3 species. *Planta* **149**, 78–90.

Fraser, C. J. D., Roulet, N. T. and Lafleur, M. 2001. Groundwater flow patterns in a large peatland. *Journal of Hydrology* **246**, 142–154.

Friend, A. D., Stevens, A. K., Knox, R. G. and Cannell, M. G. R. 1997. A process-based, terrestrial biosphere model of ecosystem dynamics (Hybrid v3.0). *Ecological Modelling* **95**, 249–287.

Frolking, S. E., Bubier, J. L., Moore, T. R., Ball, T., Bellisario, L. M., Bhardwaj, A., Carroll, P., Crill, P. M., Lafleur, P. M., Mccaughey, J. H., Roulet, N. T., Suyker, A. E., Verma, S. B., Waddington, J. M. and Whiting, G. J. 1998. Relationship between ecosystem productivity and photosynthetically active radiation for northern peatlands. *Global Biogeochemical Cycles* **12**, 115–126.

Frolking, S., Roulet, N. T., Moore, T. R., Richard, P. J. H., Lavoie, M. and Muller, S. D. 2001. Modeling northern peatland decomposition and peat accumulation. *Ecosystems* **4**, 479–498.

Frolking, S., Roulet, N. T., Moore, T. R., Lafleur, P. M., Bubier, J. L. and Crill, P. M. 2002. Modeling seasonal to annual carbon balance of mer bleue bog, Ontario, Canada. *Global Biogeochemical Cycles* **16**(3): DOI:10. 1029/2001GB001457.

Funk, D. W., Pullman, E. R., Peterson, K. M., Crill, P. M. and Billings, W. D. 1994. Influence of water-table on carbon-dioxide, carbon-monoxide, and methane fluxes from taiga bog microcosms. *Global Biogeochemical Cycles* **8**, 271–278.

Gagnon, A. S. and Gough, W. A. 2002. Hydro-climatic trends in the Hudson Bay region, Canada. *Canadian Water Resources Journal* **27**, 245–262.

Gorham, E. 1995. The biogeochemistry of northern petalands and its possible response to global warming. In: *Biotic feedbacks in the global climatic system: will the warming feed the warming*? (eds. G. M. Woodwell and F. T. Mackenzie). Oxford University Press, New York, 169–187.

Gough, W. A. and Wolfe, E. 2001. Climate change scenarios for Hudson Bay, Canada, from general circulation models. *Arctic* **54**, 142–148.

Grayson, R. B., Western, A. W., Chiew, F. H. S. and Bloschl, G. 1997. Preferred states in spatial soil moisture patterns: local and nonlocal controls. *Water Resources Research* **33**, 2897–2908.

Griffis, T. J., Black, T. A., Morgenstern, K., Barr, A. G., Nesic, Z., Drewitt, G. B., Gaumont-Guay, D. and Mccaughey, J. H. 2003. Ecophysiological controls on the carbon balances of three southern boreal forests. *Agricultural and Forest Meteorology* **117**, 53–71.

Harris, P. P., Huntingford, C., Cox, P. M., Gash, J. H.C. and Malhi, Y. 2004. Effect of soil moisture on canopy conductance of amazonian rainforest. *Agricultural and Forest Meteorology* **122**, 215–227.

Haxeltine, A. and Prentice, I. C. 1996. Biome3: an equilibrium terrestrial biosphere model based on ecophysiological constraints, resource availability, and competition among plant functional types. *Global Biogeochemical Cycles* **10**, 693–709.

Humphreys, E. R., Black, T. A., Ethier, G. J., Drewitt, G. B., Spittlehouse, D. L., Jork, E. M., Nesic, Z. and Livingston, N. J. 2003. Annual and seasonal variability of sensible and latent heat fluxes above a coastal douglas-fir forest, British Columbia, Canada. *Agricultural and Forest Meteorology* **115**, 109–125.

Humphreys, E. R., Lafleur, P. M., Admiral, S. W. and Roulet, N. T. 2004. Contrasting the interannual variability in net ecosystem exchange of carbon dioxide in a northern peatland with the variability observed in northern forests. In: *Proceedings of the 26th Conference on Agricultural and Forest Meteorology, August 23–27, Vancouver, BC, Canada*. American Meteorology Society, Boston, MA, P1. 20, 5 pp.

Jackson, R. B., Canadell, J., Ehleringer, J. R., Mooney, H. A., Sala, O. E. and Schulze, E. D. 1996. A global analysis of root distributions for terrestrial biomes. *Oecologia* **108**, 389–411.

Jarvis, P. G. 1976. Interpretation of variations in leaf water potential and stomatal conductance found in canopies in field. *Philosophical Transactions of the Royal Society of London, Series B: Biological Sciences* **273**, 593–610.

Jarvis, P. G., Massheder, J. M., Hale, S. E., Moncrieff, J. B., Rayment, M. and Scott, S. L. 1997. Seasonal variation of carbon dioxide, water vapors, and energy exchanges of a boreal black spruce forest. *Journal of Geophysical Research-Atmospheres* **102**, 28 953–28 966.

Ju, W. M. and Chen, J. M. 2005. Distribution of soil carbon stocks in canada's forests and wetlands simulated based on drainage class, topography and remotely sensed vegetation parameters. *Hydrological Processes* **19**, 77–94.

Kljun, N., Black, T. A., Griffis, T. J., Barr, A. G., Gaumont-Guay, D., Morgenstern, K., McCaughey, J. H. and Nesic, Z. 2004. Net carbon exchange of three boreal forests during a drought. In: *Proceedings of the 26th Conference on Agricultural and Forest Meteorology*, August 23–27, Vancouver, BC, Canada. American Meteorology Society, Boston, MA, P4.5, 4 pp.

Kochy, M. and Wilson, S. D. 2001. Nitrogen deposition and forest expansion in the northern great plains. *Journal of Ecology* **89**, 807–817.

Kucharik, C. J., Foley, J. A., Delire, C., Fisher, V. A., Coe, M. T., Lenters, J. D., Young-Molling, C., Ramankutty, N., Norman, J. M. and Gower, S. T. 2000. Testing the performance of a dynamic global ecosystem model: water balance, carbon balance, and vegetation structure. *Global Biogeochemical Cycles* **14**, 795–825.

Lacelle, B. 1998. Canada's soil organic carbon database. In: *Soil Processes and the Carbon Cycle* (eds. R. Lal, M. Kimble, F. Follett and B. A. Stewart). CRC Press, Boca Raton, 93–101.

Lafleur, P. M., Roulet, N. T., Bubier, J. L., Frolking, S. and Moore, T. R. 2003. Interannual variability in the peatland-atmosphere carbon dioxide exchange at an ombrotrophic bog. *Global Biogeochemical Cycles* **17**(2), 1036, DOI: 10. 1029/2002GB001983.

Letts, M. G., Roulet, N. T., Comer, N. T., Skarupa, M. R. and Verseghy, D. L. 2000. Parametrization of peatland hydraulic properties for the Canadian land surface scheme. *Atmosphere-Ocean* **38**, 141–160.

Lhomme, J. P., Elguero, E., Chehbouni, A. and Boulet, G. 1998. Stomatal control of transpiration: examination of monteith's formulation of canopy resistance. *Water Resources Research* **34**, 2301–2308.

Liu, J., Chen, J. M., Cihlar, J. and Chen, W. 1999. Net primary productivity distribution in the boreas region from a process model using satellite and surface data. *Journal of Geophysical Research* **104**(D22), 27 735–27 754.

Liu, J., Chen, J. M., Cihlar, J. and Chen, W. 2002. Net primary productivity mapped for Canada at 1-km resolution. *Global Ecology and Biogeography* **11**, 115–129.

Lloyd, J. and Taylor, J. A. 1994. On the temperature-dependence of soil respiration. *Functional Ecology* **8**, 315–323.

McGuire, A. D., Melillo, J. M., Joyce, L. A., Kicklighter, D. W., Grace, A. L., More III, B. and Vorosmarty, C. J. 1992. Interactions between carbon and nitrogen dynamics in estimating net primary productivity for potential vegetation in northern America. *Global Biogeochemical Cycles* **6**, 101–124.

Monteith, J. L. and Unsworth, M. H. 1990. *Principles of Environmental Physics*. Edward Arnold, London, 225–230.

Moore, T. R. and Knowles, R. 1989. The influence of water-table levels on methane and carbon-dioxide emissions from peatland soils. *Canadian Journal of Soil Science* **69**, 33–38.

Moore, I. D., Burch, G. J. and Mackenzie, D. H. 1988. Topographic effects on the distribution of surface soil-water and the location of

ephemeral gullies. *Transactions of the American Society of Agriculture Engineering* **31**, 1098–1107.

Moore, T. R., Roulet, N. T. and Waddington, J. M. 1998. Uncertainty in predicting the effect of climatic change on the carbon cycling of Canadian peatlands. *Climatic Change* **40**, 229–245.

Neilson, R. P. 1995. A model for predicting continental-scale vegetation distribution and water-balance. *Ecological Applications* **5**, 362–385.

Neilson, R. P. and Marks, D. 1994. A global perspective of regional vegetation and hydrologic sensitivities from climatic-change. *Journal of Vegetation Science* **5**, 715–730.

New, M., Hulme, M. and Jones, P. 1999. Representing twentieth-century space-time climate variability, Part I: development of a 1961-90 mean monthly terrestrial climatology. *Journal of Climate* **12**, 829–856.

New, M., Hulme, M. and Jones, P. 2000. Representing twentieth-century space-time climate variability. part ii: development of 1901-96 monthly grids of terrestrial surface climate. *Journal of Climate* **13**, 2217–2238.

Oechel, W. C., Hastings, S. J., Vourlitis, G., Jenkins, M., Riechers, G. and Grulke, N. 1993. Recent change of arctic tundra ecosystems from a net carbon-dioxide sink to a source. *Nature* **361**, 520–523.

Parton, W. J., Schimel, D. S., Cole, C. V. and Ojima, D. S. 1987. Analysis of factors controlling soil organic-matter levels in great-plains grasslands. *Soil Science Society of America Journal* **51**, 1173–1179.

Parton, W. J., Scurlock, J. M.O., Ojima, D. S., Gilmanov, T. G., Scholes, R. J., Schimel, D. S., Kirchner, T., Menaut, J. C., Seastedt, T., Moya, E. G., Kamnalrut, A. and Kinyamario, J. I. 1993. Observations and modeling of biomass and soil organic-matter dynamics for the grassland biome worldwide. *Global Biogeochemical Cycles* **7**, 785–809.

Paul, K. I., Polglase, P. J., Smethurst, P. J., O'connell, A. M., Carlyle, C. J. and Khanna, P. K. 2004. Soil temperature under forests: a simple model for predicting soil temperature under a range of forest types. *Agricultural and Forest Meteorology* **121**, 167–182.

Potter, C. S. 1997. An ecosystem simulation model for methane production and emission from wetlands. *Global Biogeochemical Cycles* **11**, 495–506.

Potter, C. S. 1999. Terrestrial biomass and the effects of deforestation on the global carbon cycle—results from a model of primary production using satellite observations. *Bioscience* **49**, 769–778.

Potter, C. S., Randerson, J. T., Field, C. B., Matson, P. A., Vitousek, P. M., Mooney, H. A. and Klooster, S. A. 1993. Terrestrial ecosystem production—a process model-based on global satellite and surface data. *Global Biogeochemical Cycles* **7**, 811–841.

Potter, C., Davidson, E., Nepstad, D. and De Carvalho, C. R. 2001. Ecosystem modeling and dynamic effects of deforestation on trace gas fluxes in amazon tropical forests. *Forest Ecology and Management* **152**, 97–117.

Qiu, Y., Fu, B. J., Wang, J. and Chen, L. D. 2001. Soil moisture variation in relation to topography and land use in a hillslope catchment of the loess plateau, china. *Journal of Hydrology* **240**, 243–263.

Raich, J. W., Rastetter, E. B., Melillo, J. M., Kicklighter, D. W., Steudler, P. A., Peterson, B. J., Grace, A. L., Moore, B. and Vorosmarty, C. J. 1991. Potential net primary productivity in South-America—application of a global-model. *Ecological Applications* **1**, 399–429.

Rapalee, G., Trumbore, S. E., Davidson, E. A., Harden, J. W. and Veldhuis, H. 1998. Soil carbon stocks and their rates of accumulation and loss in a boreal forest landscape. *Global Biogeochemical Cycles* **12**, 687–701.

Ro, C., Vet, R., Ord, D. and Holloway, A. 1995. National Atmospheric Chemistry Database 1993 annual report, acid precipitation in eastern Northern America. Atmospheric Environment Service, Environment Canada.

Rodriguez-Iturbe, I. 2000. Ecohydrology: a hydrologic perspective of climate-soil-vegetation dynamics. *Water Resources Research* **36**, 3–9.

Roulet, N. T., Munro, D. S. and Mortsch, L. 1997. Wetlands. In: *The Surface Climate of Canada* (eds. W. G. Baily, T. R. Oke, W. R. Rouse). McGill-Queen's University Press, Montreal, 149–171.

Running, S. W. and Gower, S. T. 1991. Forest-BGC, a general-model of forest ecosystem processes for regional applications, II, dynamic carbon allocation and nitrogen budgets. *Tree Physiology* **9**, 147–160.

Saulnier, G. M., Obled, C. and Beven, K. 1997. Analytical compensation between dtm grid resolution and effective values of saturated hydraulic conductivity within the topmodel framework. *Hydrological Processes* **11**, 1331–1346.

Saxton, K. E., Rawls, W. J., Romberger, J. S. and Papendick, R. I. 1986. Estimating generalized soil-water characteristics from texture. *Soil Science Society of America Journal* **50**, 1031–1036.

Schut, P., Shields, J., Tarnocai, C., Coote, D. and Marshall, I. 1994. Soil Landscapes of Canada-an environmental reporting tool. In: *Canadian Conference on GIS Proceedings*, 6-10 June, Ottawa, 953–965.

Sellers, P. J., Mintz, Y., Sud, Y. C. and Dalcher, A. 1986. A simple biosphere model (SiB) for use within general-circulation models. *Journal of the Atmospheric Sciences* **43**, 505–531.

Sellers, P. J., Randall, D. A., Collatz, G. J., Berry, J. A., Field, C. B., Dazlich, D. A., Zhang, C., Collelo, G. D. and Bounoua, L. 1996. A revised land surface parameterization (SiB2) for atmospheric GCMs. part I. model formulation. *Journal of Climate* **9**, 676–705.

Silvola, J., Alm, J., Ahlholm, U., Nykanen, H. and Martikainen, P. J. 1996. CO_2 fluxes from peat in boreal mires under varying temperature and moisture conditions. *Journal of Ecology* **84**, 219–228.

Soegaard, H. and Nordstroem, C. 1999. Carbon dioxide exchange in a high-arctic fen estimated by eddy covariance measurements and modelling. *Global Change Biology* **5**, 547–562.

Soulis, E. D., Snelgrove, K. R., Kouwen, N., Seglenieks, F. and Verseghy, D. L. 2000. Towards closing the vertical water balance in canadian atmospheric models: coupling of the land surface scheme class with the distributed hydrological model watflood. *Atmosphere-Ocean* **38**, 251–269.

Su, M., Stolte, W. J. and Van Der Kamp, G. 2000. Modelling Canadian prairie wetland hydrology using a semi-distributed streamflow model. *Hydrological Processes* **14**, 2405–2422.

Tarnocai, C. 1998. The amount of organic carbon in various soil orders and ecological provinces in Canada. In: *Soil Processes and the Carbon Cycle* (eds. R. Lal, M. Kimble, F. Follett and B. A. Stewart). CRC Press, Boca Raton, 81–92.

Thompson, S. L. and Pollard, D. 1995. A global climate model (GENESIS) with a land-surface transfer scheme (LSX). Part I: Present climate simulation. *Journal of Climate* **8**, 732–761.

Thornton, P. E. and Running, S. W. 1999. An improved algorithm for estimating incident daily solar radiation from measurements of temperature, humidity, and precipitation. *Agricultural and Forest Meteorology* **93**, 211–228.

Tolonen, K., Vasamder, H., Damman, A. W. H. and Clymo, R. S. 1992. Preliminary estimate of long-term c accumulation and loss in 25 boreal peatlands. *Suo* **43**, 277–280.

Trumbore, S. E. and Harden, J. W. 1997. Accumulation and turnover of carbon in organic and mineral soils of the boreas northern study area. *Journal of Geophysical Research* **102**(D4), 28 817–28 830.

Turunen, J., Roulet, N. T., Moore, T. R. and Richard, P. J.H. 2004. Nitrogen deposition and increased carbon accumulation in ombrotrophic peatlands in eastern Canada. *Global Biogeochemical Cycles* **18**, DOI: 10. 1029/2003GB002154.

Turunen, J., Tomppo, E., Tolonen, K. and Reinikainen, A. 2002. Estimating carbon accumulation rates of undrained mires in finland—application to boreal and subarctic regions. *Holocene* **12**, 69–80.

Waddington, J. M., Griffis, T. J. and Rouse, W. R. 1998. Northern Canadian wetlands: net ecosystem co2 exchange and climatic change. *Climatic Change* **40**, 267–275.

Western, A. W., Grayson, R. B., Bloschl, G., Willgoose, G. R. and Mcmahon, T. A. 1999. Observed spatial organization of soil moisture and its relation to terrain indices. *Water Resources Research* **35**, 797–810.

White, A., Cannell, M. G.R. and Friend, A. D. 2000. The high-latitude terrestrial carbon sink: a model analysis. *Global Change Biology* **6**, 227–245.

Wigmosta, M. S., Vail, L. W. and Lettenmaier, D. P. 1994. A distributed hydrology-vegetation model for complex terrain. *Water Resources Research* **30**, 1665–1679.

Query

Journal: TEB
Paper: teb168

Dear Author

During the copy-editing of your paper, the following queries arose. Please respond to these by marking up your proofs with the necessary changes/additions. Please write your answers on the query sheet if there is insufficient space on the page proofs. Please write clearly and follow the conventions shown on the corrections sheet. If returning the proof by fax do not write too close to the paper's edge. Please remember that illegible mark-ups may delay publication.

Query Reference	Query	Remarks
Q1	Author: Please confirm correctness of suggested running head.	

MARKED PROOF

Please correct and return this set

Please use the proof correction marks shown below for all alterations and corrections. If you wish to return your proof by fax you should ensure that all amendments are written clearly in dark ink and are made well within the page margins.

Instruction to printer	Textual mark	Marginal mark
Leave unchanged	⋯ under matter to remain	Stet
Insert in text the matter indicated in the margin	⅄	New matter followed by ⅄
Delete	⊢⊣ through matter to be deleted	⌀
Delete and close up	⊖ through matter to be deleted	⌀
Substitute character or substitute part of one or more word(s)	/ through letter or ⊢⊣ through word	New letter or new word
Change to italics	— under matter to be changed	⊔⊔⌡
Change to capitals	≡ under matter to be changed	≡
Change to small capitals	═ under matter to be changed	=
Change to bold type	∼∼ under matter to be changed	∼∼
Change to bold italic	≈ under matter to be changed	≈⌡
Change to lower case	Encircle matter to be changed	≢
Change italic to upright type	(As above)	⊔⌡
Insert 'superior' character	/ through character or ⅄ where required	⅄ under character e.g. ⅄
Insert 'inferior' character	(As above)	⅄ over character e.g. ⅄
Insert full stop	(As above)	⊙
Insert comma	(As above)	,
Insert single quotation marks	(As above)	⅄ and/or ⅄
Insert double quotation marks	(As above)	⅄ and/or ⅄
Insert hyphen	(As above)	⊝
Start new paragraph	⌐	⌐
No new paragraph	⌇	⌇
Transpose	⊔⌐⌐	⊔⌐⌐
Close up	linking ⊃ letters	⊃
Insert space between letters	⅄ between letters affected	#
Insert space between words	⅄ between words affected	#
Reduce space between letters	⊤ between letters affected	⊤
Reduce space between words	⊤ between words affected	⊤